An Indirect Rotor Position Estimation Technique for a Fault-Tolerant Brushless PM Motor Drive

J. S. An, N. Ertugrul, W. L. Soong, J. Zhu, and A. Gargoom

School of Electrical and Electronic Engineering, University of Adelaide, Adelaide, 5005, Australia

Abstract - **This paper proposes an indirect rotor position estimation method for a fault-tolerant brushless PM motor drive that has a dual motor module on a common shaft. The technique is based on flux linkage increments of phase windings and performing multiple rotor position estimations using pairs of phases in the motor drive. The paper provides the theory of the method and presents extensive test results to demonstrate its effectiveness using off line real data obtained under various practical operating conditions including faulty states and parameter variations.**

I. INTRODUCTION

Unlike conventional three phase motor configurations, fault-tolerant motor drives should continue to operate under partial failures of motor, sensors or inverter. In some of the recent studies, permanent magnet (PM) AC motors with fault-tolerant winding configurations (with electrically isolated and magnetically decoupled windings) driven by independent H-bridge inverters were utilized as they offer excellent torque density and efficiency [1, 2]. In addition, parallel redundancy was introduced in such motor drives by utilizing multiple motor modules on a common shaft [2]. However, in a practical system it is important to consider redundancy and fault tolerant operation for every critical section of the entire system.

As it is well known, the rotor position sensor is one of the most critical sections in brushless PM AC motor drives. Resolvers, encoders or hall-effect based sensors are commonly used in such drives primarily for phase current commutation. However, using a single rotor position sensor in a fault-tolerant motor drive can reduce the reliability of the system significantly. Moreover, such direct position sensors can be expensive and they are sensitive to environmental factors. Furthermore, since the direct position sensors require additional signal wiring between the motor and its controller, the reliability is reduced further. Therefore, there is a need for an indirect position estimation method to increase the reliability of the drive while offering redundancy for rotor position information specifically in the case of a fault.

A sensorless position estimation method for a six-phase fault-tolerant PM AC motor drive for an aircraft fuel pump was discussed in [3]. However, this method has limitations under low speed operation due to integration drift which are only partially addressed by clamping the flux linkage estimates to the known maximum values.

To improve reliability and to offer parallel redundancy for the rotor position estimation in a fault tolerant motor drive, a motor model-based indirect position estimation method based on flux-linkage increments was presented in [4]. This early study provided some computer simulation studies without examining its performance under real

operating conditions. This paper aims to address this by implementing the entire drive system and utilizing real measurements from the drive system to be able to estimate the rotor position accurately. As the method proposed is based on the rotor position estimation using a pair of motor phases only, the redundancy on the rotor position has been increased significantly.

In this paper, the principle of the proposed indirect method is explained in details first. Then the entire experimental setup including the fault-tolerant brushless PM AC motor modules and the inverters is explained, which is followed by the data acquisition system for off-line real data capturing. Finally, the paper presents extensive experimental results under various practical operating conditions to verify its effectiveness.

II. PRINCIPLE OF INDIRECT ROTOR POSITION ESTIMATION

The paper utilizes two three-phase brushless PM AC motor modules on a common shaft. Therefore, the phase windings of each motor module can be modeled by a series electrical circuit containing a resistance, an inductance and a sinusoidal back-EMF voltage source. Since the motors are surface-mounted PM machines and their phase windings are magnetically isolated utilizing concentrated windings, it is assumed that the winding inductance is a constant self inductance.

Hence, the voltage equations of the entire fault tolerant motor drive with two identical motor modules can be given as

$$\begin{bmatrix} v_{ai} \\ v_{bi} \\ v_{ci} \end{bmatrix} = \begin{bmatrix} R & 0 & 0 \\ 0 & R & 0 \\ 0 & 0 & R \end{bmatrix} \begin{bmatrix} i_{ai} \\ i_{bi} \\ i_{ci} \end{bmatrix} + \begin{bmatrix} L & 0 & 0 \\ 0 & L & 0 \\ 0 & 0 & L \end{bmatrix} \frac{d}{dt} \begin{bmatrix} i_{ai} \\ i_{bi} \\ i_{ci} \end{bmatrix},$$
$$+ \frac{k_e}{p} \cdot \frac{d\theta}{dt} \begin{bmatrix} e_{ai}(\theta) \\ e_{bi}(\theta) \\ e_{ci}(\theta) \end{bmatrix}, \qquad i=1,2 \tag{1}$$

where v_{ai}, v_{bi}, and v_{ci} are the phase voltages; i_{ai}, i_{bi} and i_{ci} are the phase currents, R is the winding resistance and L denotes the self inductance of the windings. The subscript i in the equations represents the number of motor modules. The last term on the right hand side of (1) represents the back-EMF voltages of the windings, where k_e is the back-EMF constant, θ is the electrical rotor angle, p is the number of pole pairs, and $e_{ai}(\theta)$, $e_{bi}(\theta)$ and $e_{ci}(\theta)$ are unit-magnitude sinusoidal back-EMF functions that

1553

are 120° out of phase. It should be noted here that two motor modules are mechanically aligned. Therefore, the back-EMF functions of the motor modules are assumed to be in phase.

Assuming that the sampling time is small enough in (1), the estimated rotor position increments of all phases can be derived in discrete form as a function of the phase flux linkage increments as given below

$$
\begin{bmatrix} \Delta\theta_{ai} \\ \Delta\theta_{bi} \\ \Delta\theta_{ci} \end{bmatrix} = \frac{p}{k_e} \begin{bmatrix} \dfrac{(v_{ai} - Ri_{ai}) \cdot \Delta t - L\Delta i_{ai}}{e_{ai}(\theta)} \\ \dfrac{(v_{bi} - Ri_{bi}) \cdot \Delta t - L\Delta i_{bi}}{e_{bi}(\theta)} \\ \dfrac{(v_{ci} - Ri_{ci}) \cdot \Delta t - L\Delta i_{ci}}{e_{ci}(\theta)} \end{bmatrix} = \frac{p}{k_e} \begin{bmatrix} \dfrac{\Delta\psi_{ai}}{e_{ai}(\theta)} \\ \dfrac{\Delta\psi_{bi}}{e_{bi}(\theta)} \\ \dfrac{\Delta\psi_{ci}}{e_{ci}(\theta)} \end{bmatrix}. \quad (2)
$$

Here $\Delta\theta_{ai}$, $\Delta\theta_{bi}$, and $\Delta\theta_{ci}$ are the electrical rotor position increments for every phase, Δi_{ai}, Δi_{bi}, and Δi_{ci} are the phase current increments, $\Delta\psi_{ai}$, $\Delta\psi_{bi}$ and $\Delta\psi_{ci}$ are the phase flux linkage increments, and Δt is the sampling time.

As can be seen in (2), the estimated rotor position increments are directly proportional to the phase flux linkage increments and inversely proportional to the unit-magnitude sinusoidal back-EMF functions of corresponding windings. However, since the unit back-EMF functions are sinusoidal functions, they have zero-crossing regions twice every electrical cycle. Therefore, for a given flux linkage increment in these regions, the estimated rotor position increments can become very large producing a large position error.

A solution for this problem was first addressed in [5] for a conventional three-phase brushless PM AC motor (with a star-connected and tightly coupled windings), utilizing all three phase back-EMFs in the denominator of the position increments.

To overcome the above described large position errors in the zero-crossing regions of the back-EMF functions of the fault tolerant motor drive, the method described in [5] has been modified. In this paper, both sides of (1) are multiplied by the squared back-EMF functions of the corresponding phases ($e^2_{ai}(\theta)$, $e^2_{bi}(\theta)$ and $e^2_{ci}(\theta)$ respectively). The resulting equations of all neighbouring phases (phases a-b, b-c, and c-a) are then summed together to obtain multiple rotor position increments for each pair of the phases of the motor drive as given below

$$
\begin{bmatrix} \Delta\theta_{abi} \\ \Delta\theta_{bci} \\ \Delta\theta_{cai} \end{bmatrix} = \frac{p}{k_e} \begin{bmatrix} \dfrac{\Delta\Psi_{ai}e_{ai} + \Delta\Psi_{bi}e_{bi}}{e^2_{ai} + e^2_{bi}} \\ \dfrac{\Delta\Psi_{bi}e_{2i} + \Delta\Psi_{ci}e_{ci}}{e^2_{bi} + e^2_{ci}} \\ \dfrac{\Delta\Psi_{ci}e_{3i} + \Delta\Psi_{ai}e_{ai}}{e^2_{ci} + e^2_{ai}} \end{bmatrix}, \quad (3)
$$

where $\Delta\theta_{abi}$, $\Delta\theta_{bci}$, and $\Delta\theta_{cai}$ are the position increments obtained by using pairs of the phases, a-b, b-c, and c-a, respectively.

As it can be observed in (3), since the sinusoidal back-EMF functions of neighbouring phases are out of phase 120° electrical, the denominators in (3) are always greater than 0.5, which prevents the large incremental position estimation errors in the zero-crossing regions of the phase back-EMF functions.

The estimated rotor position increments in (3) can be utilised to predict the rotor position in the motor drive by using both the estimated rotor position increments and the values obtained in the previous sampling interval as given below.

$$
\begin{bmatrix} \theta^*_{abi}(k) \\ \theta^*_{bci}(k) \\ \theta^*_{cai}(k) \end{bmatrix} = \begin{bmatrix} \theta_{abi}(k-1) + \Delta\theta_{abi} \\ \theta_{bci}(k-1) + \Delta\theta_{bci} \\ \theta_{cai}(k-1) + \Delta\theta_{cai} \end{bmatrix}, \quad (4)
$$

where, k is an integer representing at the k-th sampling instant, $\theta^*_{abi}(k)$, $\theta^*_{bci}(k)$ and $\theta^*_{cai}(k)$ are the predicted rotor positions and $\theta_{abi}(k-1)$, $\theta_{bci}(k-1)$ and $\theta_{cai}(k-1)$ are the estimated rotor positions at the previous sampling instant.

In an ideal system, this simple integration method in (4) can be used to estimate the rotor position. However, there are large steady-state errors in a practical system, which are primarily due to the finite sampling frequency, measurement errors and parameter variations. These errors can accumulate during the integration and consequently producing significant position errors.

To compensate the steady-state position errors mentioned above, a phase-locked loop (PLL) technique in [6] was also adopted in the paper, which is later modified to lock the predicted rotor position to the phase of the flux linkage increments.

The PLL technique in this paper utilizes the fact that the back-EMF function is proportional to the rate of change of flux linkage and hence the flux linkage increment. Thus the back-EMF functions using the predicted rotor positions should be in phase with the measured flux linkage increments.

The block diagram of position estimation technique is illustrated in Fig. 1 for a pair of phase windings. As shown in the figure, both the voltage and the current values are measured to calculate the flux linkage increments, which becomes an input to the position estimation block. In the PLL technique, the flux linkage increments and the back-EMF functions are used as inputs to the phase detector, which are given in the equation below.

1554

$$\begin{bmatrix} \left\| \vec{e} \times \Delta \vec{\psi} \right\|_{abi} \\ \left\| \vec{e} \times \Delta \vec{\psi} \right\|_{bci} \\ \left\| \vec{e} \times \Delta \vec{\psi} \right\|_{cai} \end{bmatrix} = \begin{bmatrix} e_{ai}(\theta_{abi}^*)\Delta\psi_{bi} - e_{bi}(\theta_{abi}^*)\Delta\psi_{ai} \\ e_{bi}(\theta_{bci}^*)\Delta\psi_{ci} - e_{ci}(\theta_{bci}^*)\Delta\psi_{bi} \\ e_{ci}(\theta_{cai}^*)\Delta\psi_{ai} - e_{ai}(\theta_{cai}^*)\Delta\psi_{ci} \end{bmatrix}$$

$$= \frac{\sqrt{3}}{2} \begin{bmatrix} |\Delta\psi|\sin(\theta_{fabi} - \theta_{abi}^*) \\ |\Delta\psi|\sin(\theta_{fbci} - \theta_{bci}^*) \\ |\Delta\psi|\sin(\theta_{fcai} - \theta_{cai}^*) \end{bmatrix} \approx \begin{bmatrix} K_{abi}(\theta_{fabi} - \theta_{abi}^*) \\ K_{bci}(\theta_{fbci} - \theta_{bci}^*) \\ K_{cai}(\theta_{fcai} - \theta_{cai}^*) \end{bmatrix} \cdot \qquad (5)$$

$$= \begin{bmatrix} K_{abi}\delta\theta_{abi} \\ K_{bci}\delta\theta_{bci} \\ K_{cai}\delta\theta_{cai} \end{bmatrix}, \quad where \begin{pmatrix} \Delta\psi_{ai} = |\Delta\psi| \cdot e_{ai}(\theta_{Fi}) \\ \Delta\psi_{bi} = |\Delta\psi| \cdot e_{bi}(\theta_{Fi}) \\ \Delta\psi_{ci} = |\Delta\psi| \cdot e_{ai}(\theta_{Fi}) \end{pmatrix}$$

Here, θ_{fabi}, θ_{fbci} and θ_{fcai} are the phase angles of the flux linkage increments, K_{abi}, K_{bci}, and K_{cai}, are the gains of the phase detectors, $\delta\theta_{abi}$, $\delta\theta_{bci}$ and $\delta\theta_{cai}$ are the phase differences between the flux linkage increments and the predicted rotor positions, and $|\Delta\psi|$ is the amplitude of the flux linkage increments.
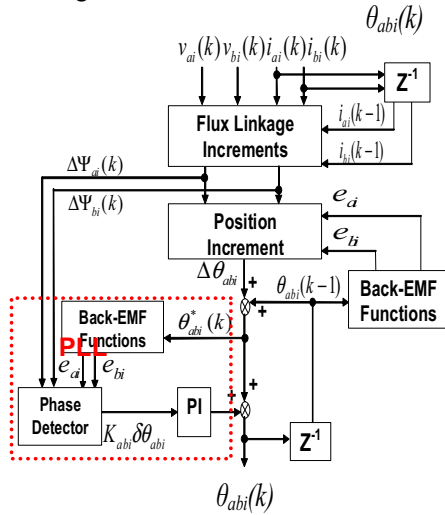

Figure 1. Block diagram of the indirect rotor position estimator using a pair of phases, *a-b*.

The phase detector in Fig.1 performs a vector product to produce an output proportional to the phase difference between the phase angle of the flux linkage increments and the predicted rotor position. The output of the phase detector is fed into a proportional integral (PI) regulator, which is then added to the predicted rotor position to compensate for the steady state errors as given in (6). This method enables the estimated rotor position to follow the phase of the flux linkage increments with a very small phase difference. Based on the above explanations, the rotor position estimates between the phases *a-b*, *b-c* and *c-a* of two motor modules can be given by

$$\begin{bmatrix} \theta_{abi}(k) \\ \theta_{bci}(k) \\ \theta_{cai}(k) \end{bmatrix} = \begin{bmatrix} \theta_{abi}^*(k) + K_p K_{abi}\delta\theta_{abi}(k) + K_i \sum_{n=0}^{k} K_{abi}\delta\theta_{abi}(n) \\ \theta_{bci}^*(k) + K_p K_{bci}\delta\theta_{bci}(k) + K_i \sum_{n=0}^{k} K_{bci}\delta\theta_{bci}(n) \\ \theta_{cai}^*(k) + K_p K_{cai}\delta\theta_{cai}(k) + K_i \sum_{n=0}^{k} K_{cai}\delta\theta_{cai}(n) \end{bmatrix}, \quad (6)$$

where K_p and K_i are the proportional and integral gains of the PI regulator.

III. EXPERIMENTAL SETUP

To investigate the performance and effectiveness of the position estimation method, a fault-tolerant motor drive and a data acquisition system were implemented in this paper. The photo of the entire hardware system and its principal block diagram is given in Fig.2.
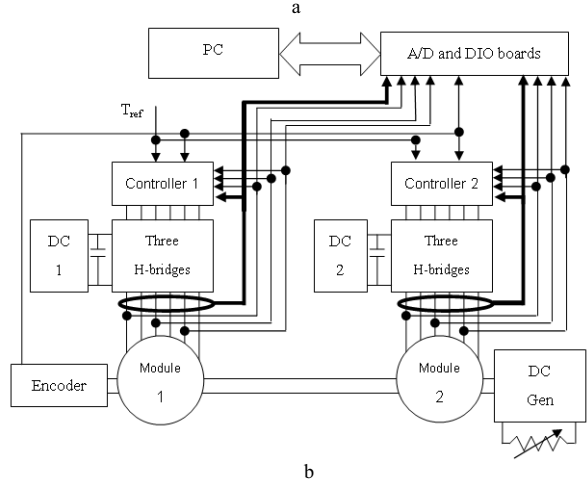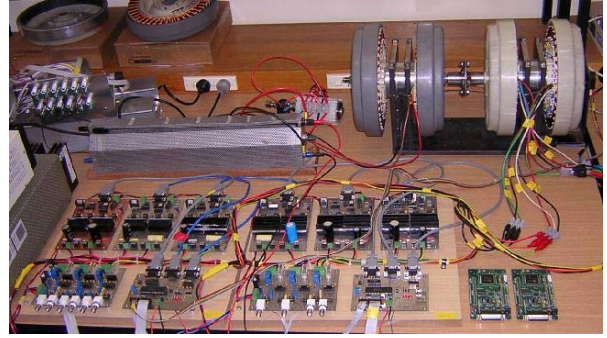

Figure 2. The photo of the experimental setup of the fault-tolerant brushless PM AC motor drive with redundancy (a) and the block diagram of the entire system including the data acquisition system (b).

As shown in Fig. 2, the fault-tolerant brushless PM motor consists of two fault-tolerant three-phase brushless PM AC motor modules on a common mechanical shaft. Each motor module has electrically isolated phases and concentrated windings providing minimum mutual coupling. Table 1 summaries some of the characteristic parameters of the motor modules.

TABLE. 1. THE MOTOR PARAMETERS

Parameters	Values
Phase resistance (*R*)	0.87 (Ω)
Phase inductance (*L*)	2.1 (mH)
Back-emf constance (k_e)	0.0896 (V/rad/s)
Number of pole pairs (*P*)	2

The phases of each motor module are driven by a separate single phase MOSFET based H-Bridge inverter, which accommodates its own isolation and driver circuits. The inverter of each motor module is controlled by a dsPIC30F40ll based controller to perform torque control.

1555

In addition, the setup includes an incremental encoder (HEDS-5640, 500 ppr) on the common shaft to be able to measure the actual rotor position and a DC generator with a variable power resistor (12.4 Ω /10A) for loading purpose. An additional power switch was also accommodated on the load side to be able to simulate the dynamic load change in the motor drive.

In order to obtain off-line data from the system, a LabVIEW based data acquisition system was also developed. In this section of the experimental setup, two high speed A/D boards (PCI-6110E, each 4-channels) and one high speed DIO board (PCI-6534) from National Instruments Inc. are utilized. All the boards are installed inside a PC and are synchronized to perform simultaneous measurements of three phase currents, three phase voltages, and the actual rotor position.

The voltage measurements were done using three high bandwidth differential probes (Model 70095, Yokogawa), and the current measurements are done through three high bandwidth current transducers (LTS15-NP, LEM).

A custom built data logging software was developed using LabVIEW graphical programming tool, which had a sampling rate of 100 kHz. The software acquired all the data as well as obtained the actual rotor position information for comparison purpose.

IV. EXPERIMENTAL RESULTS

In order to validate the feasibility of the developed indirect position estimation technique, extensive experimental tests were performed under various operation conditions. The operating conditions include starting, steady-state operation, low and high speed operation, dynamic load change, one winding-open circuit fault, single current sensor fault and single voltage sensor failure.

In the experiments, the fault-tolerant motor drive was operated in the torque control mode using hysteresis current control scheme in the controller. It should also be noted here that the controller used the encoder to perform the closed loop current control. However, the rotor position estimation algorithm in this paper utilized the off line real data to calculate the rotor position.

As stated above, the measured voltage and current data were used to estimate the rotor position indirectly, which was also performed by a custom written software in LabView. The software estimates multiple incremental rotor positions as given in (6) for pairs of phases and also calculates the actual rotor position using the incremental encoder outputs. Since there is only one rotor position data in the motor drive, the rotor position error is given reference to the average rotor position estimation that was based on the average of the multiple rotor position estimates in (6).

In the results presented, the initial value of the rotor position is assumed to be known as the initial value of the actual rotor position. Further studies will be carried out to study the effect of the incorrect initial rotor position value in the estimates. Moreover, the future studies will integrate the rotor position estimates into the controller to eliminate the encoder.

Fig. 3 shows a set of test results obtained from Module 1 during the starting of the fault tolerant motor drive. Since this test was instigated by turning on the DC link voltage supply of the inverter circuit, the measured

voltage and current waveforms of the phase windings follows the supply voltage as well as the special starting algorithm that was implemented in the actual controller.

The results in Fig. 3 illustrate the sinusoidally controlled phase current waveforms and corresponding voltage waveforms of all three phases of the motor module 1. The actual rotor position and three rotor position estimates based on (6) are also given in the figure, which is followed by the position error. As can be seen in the figure, although the error is larger at the first electrical cycle, it reduces significantly to a level (less than ±7% at steady-state speed) that is acceptable in a real motor drive.
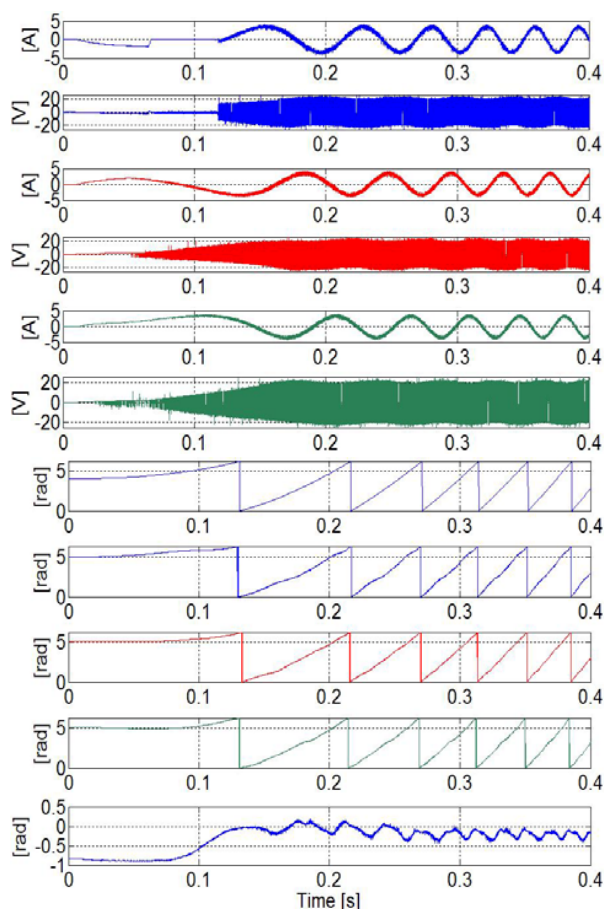

Figure 3. Starting performance of the motor Module 1 from the top: i_a, v_a, i_b, v_b, i_c, v_c, θ_{actual} (actual electrical rotor position), θ_{ab}, θ_{bc}, θ_{ca}, θ_{error} (reference to the average value of the estimated positions).

To demonstrate the steady-state performance of the indirect position estimation method, two sets of results were also obtained using the off line real data. A low speed and a high speed operation results of the motor drive are presented in Fig. 4 and Fig. 5 respectively.

It should be noted here that due to the space limitations only a single phase current and voltage waveforms are given in the figures. The results demonstrate that the rotor position estimation is satisfactory both at low and high speed operation of the motor drive (< ±5% at low speed and <±2% at high speed).
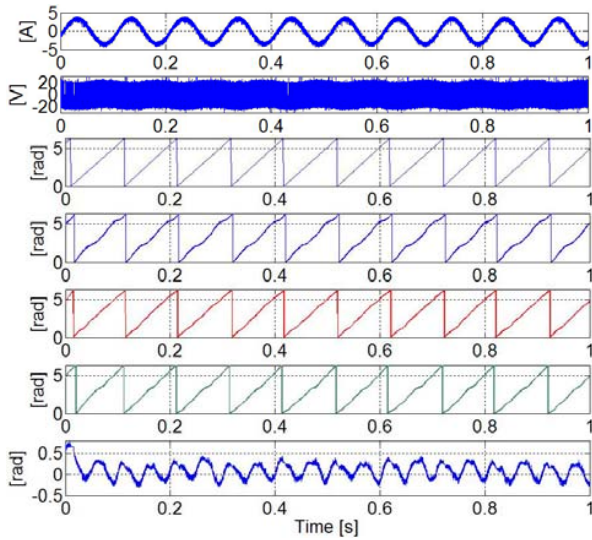
1556

Figure 4. Steady-state performance of the motor module 1 at low speed operation (300 rpm) from the top : i_a, v_a, θ_{actual} θ_{ab}, θ_{bc}, θ_{ca}, θ_{error}

Figure 6. Dynamic performance of the motor module 1 under a step load change from high speed to low speed, from the top: i_a, v_a, θ_{actual} θ_{ab}, θ_{bc}, θ_{ca}, θ_{error}.
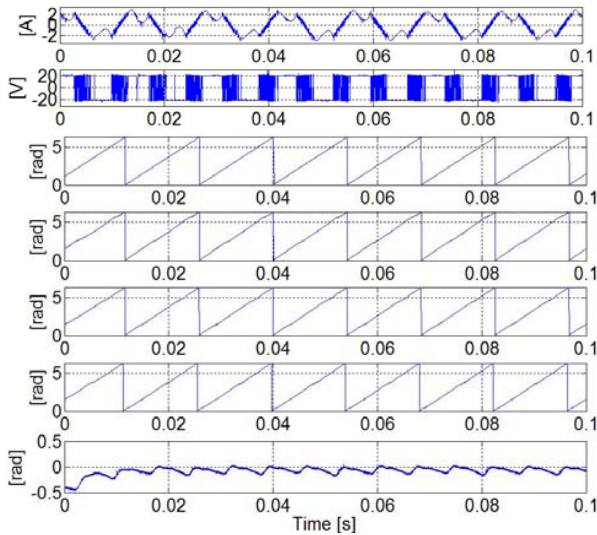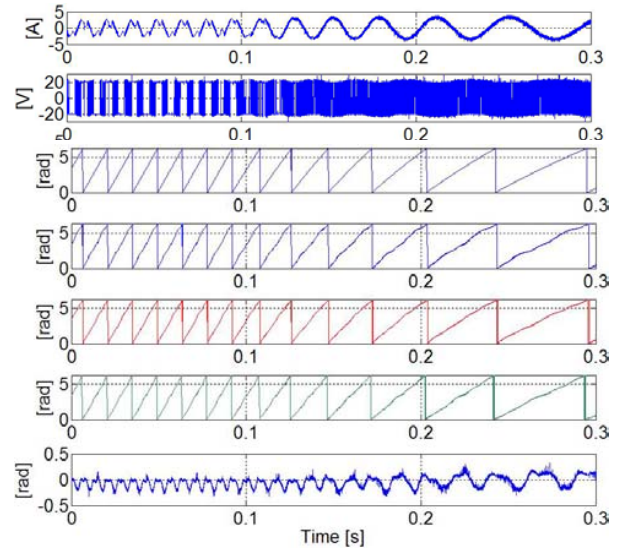

Figure 5. Steady-state performance of the motor module 1 at high speed operation (2100 rpm) from the top : i_a, v_a, θ_{actual} θ_{ab}, θ_{bc}, θ_{ca}, θ_{error}
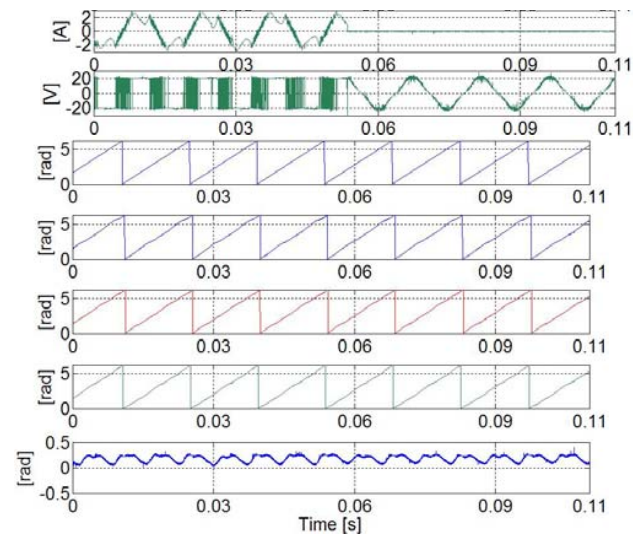

Figure 7. Performance under one-phase winding open fault in the motor module 1: i_a, v_a, θ_{actual} , θ_{ab}, θ_{bc}, θ_{ca}, θ_{error} .

Fig. 6 demonstrates a dynamic-state performance of the proposed method where a step load change is applied to the fault-tolerant motor drive during a steady-state operation of the motor by removing the resistive load connected in the dc generator. Although the position estimation errors increase slightly after a step change of a load, the error is still at acceptable levels to be utilized in a real closed-loop control.

Fig. 7 illustrates the behaviour of the position estimation method under one phase winding-open circuit fault (Phase a of Module 1). In Fig. 7, the voltage and current waveforms of the faulty phase were shown before and after the fault, and three rotor position estimates are also given using the estimations based on pairs of phases. As can be seen in these results, due to the presence of the back-EMF waveform of the open circuited phase (assuming that the fault occurred before the voltage sensor measurement points), the developed indirect estimation technique is not affected by this fault and the position estimation error is low (<±5%).

Further tests were also performed to investigate the capabilities of the method under a single current sensor fault (with a four times greater gain compared to the correct value) and a single voltage sensor fault (with one fifth of the actual correct gain). Due to the space limitations, the results are not provided in this paper. In these tests, the estimated rotor positions obtained from healthy pair of phases are found at satisfactory levels (<±3%).

Since the estimation method utilized in this paper is based on the motor model, further tests were also performed to test the capability of the estimation method under parameter changes of the motor drive. In these tests the electrical circuit parameters (resistance, inductance and back-EMF constant) were varied ±30% reference to their original values under a steady-state operating speed of 2,100 rpm. The tests revealed that the back-EMF constant variation causes larger position errors than resistance and inductance variations. However, the error in

1557

the estimated rotor position is found at the acceptable levels in all of the tests.

Fig. 8 summaries a set of test results under back-EMF constant variations of ±30% and under a steady state speed of 2100 rpm.
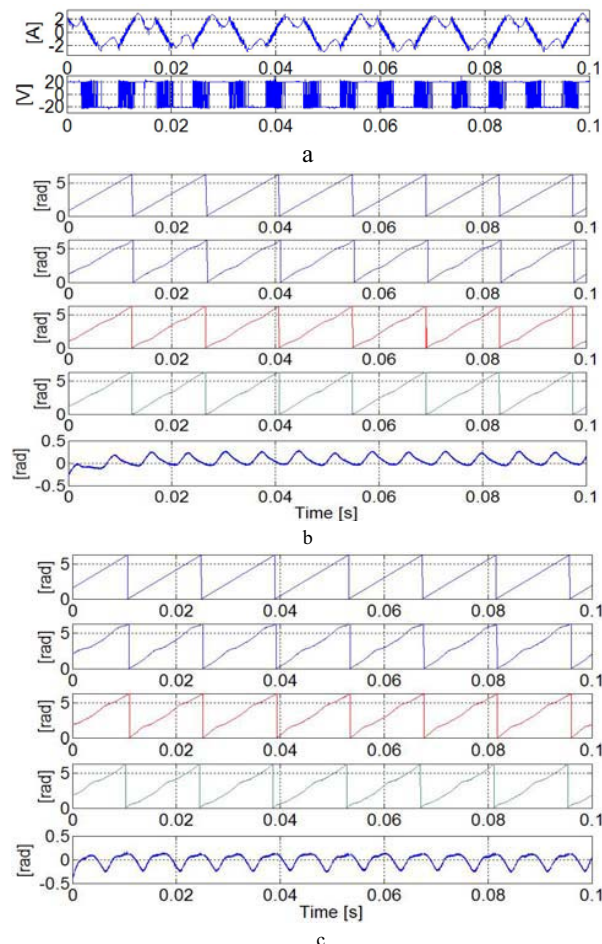

Figure 8. Performance of the motor module 1 under back-EMF constant variations of ±30% and at a speed of 2100rpm. a) Phase a voltage and current waveforms, b) θ_{actual} , θ_{ab}, θ_{bc}, θ_{ca}, θ_{error} under +30% back-EMF constant (1.3* k_e), c) θ_{actual}, θ_{ab}, θ_{bc}, θ_{ca}, θ_{error} under -30% back-EMF constant (0.7* k_e).

V. CONCLUSIONS

To be able to offer a fault tolerant motor drive system for safety critical applications such as aerospace and vehicle applications, it is important to develop fault tolerant units for every critical section of the drive system. The fault-tolerant motor drive utilized in this study was obtained using a dual three-phase surface-mounted PM AC motor modules on a common shaft, which are specially constructed to introduce magnetically and electrically isolated windings. Each phase of the motor modules was driven by an H-bridge inverter.

The paper proposed an indirect position estimation technique that is suitable for practical drives. The principal aim of the study was to improve the reliability of the drive while offering multiple redundancies for the rotor position estimation under faulty operation. In addition, measurement inaccuracies and parameter variations are also considered in the position estimation

algorithms by introducing a phase-locked loop to compensate the steady-state position errors.

The proposed method is based on the motor models of each motor module, which utilizes the current and voltage measurements from all of the phases. Using the method presented, a total of six position estimations can be done, which are based on the flux linkage increments of any two phases in a motor module.

The method provides highly redundant rotor position information. A final single rotor position estimate in a healthy motor drive can be obtained by averaging six rotor position estimates. In the case of a fault however, the rotor position estimate can utilize the data obtained from any healthy two phases of the motor module.

In order to verify the effectiveness of the proposed position estimation method for the fault-tolerant brushless PM motor drive, extensive experimental results were presented using real-time off line data. The operating conditions included in this study are: starting performance, dynamic performance, steady-state performance under slow and high speeds, operation under sensor circuit faults and winding-open circuit fault. In addition, the parameter sensitivity of the proposed method was also studied using real-time off line data under a steady state speed of 2100rpm.

It was demonstrated using the experimental results that the position estimation technique performs very well under various practical operating condition of the fault tolerant motor drive. In the test results obtained, the position error is found to be satisfactory, less than ±5%.

The future study will focus on the implementation of the entire system using a high end DSP based controller approach to be able to eliminate the direct rotor position measurement by replacing with the estimated rotor position.

REFERENCES

[1] B. C. Mecrow, A. G. Jack, J. A. Haylock, and J. Coles, "Fault-Tolerant Permanent Magnet Machine Drives," *IEE Proceedings-Electric Power Applications*, vol. 143, no. 6, pp.437-442, Nov. 1996.

[2] N. Ertugrul, W. Soong, G. Dostal, and D. Saxon, "Fault Tolerant Motor Drive System with Redundancy for Critical Applications," *in Power Electronics Specialists Conference, PESC02 2002 IEEE 33rd Annual Meeting*, vol. 3, pp.1457-1462, 23-27 June 2002.

[3] S. Green, D. J. Atkinson, A. G. Jack, B. C. Mecrow, and A. King, "Sensorless Operation of a Fault Tolerant PM Drive," *IEE Proceedings-Electric Power Appl.*, vol. 150, no. 2, pp.117-125, Mar. 2003.

[4] J. S. An, N. Ertugrul, and W. L. Soong, "Sensorless Position Estimation in a Fault Tolerant Surface-Mounted Permanent Magnet AC Motor Drive with Redundancy," *IECON'06 The 32nd Annual Conference of the IEEE Industrial Electronics Society*, Paris, France, pp.1429-1434, Nov. 6-10 2006.

[5] L. Ying and N. Ertugrul, "A Novel, Robust DSP-Based Indirect Rotor Position Estimation for Permanent Magnet AC Motors without Rotor Saliency," *IEEE Trans. On Power Electronics*, vol. 18, no. 2, pp.539-546, Mar. 2003.

[6] T. Emura, L. Wang, M. Yamanaka, and H. Nakayama, "A High-Precision Positioning Servo Controller Based on Phase/Frequency Detecting Technique of Two-Phase-Type PLL," *IEEE Trans. On Industrial Electronics*, vol. 47, no. 6, pp.1298-1306, Dec. 2000.